

Pattern formation on a sphere

P. C. Matthews

School of Mathematical Sciences, University of Nottingham, University Park, Nottingham NG7 2RD, United Kingdom

(Received 10 December 2002; published 24 March 2003)

Pattern formation on the surface of a sphere is described by equations involving interactions of spherical harmonics of degree l . When l is even, the leading-order equations are determined uniquely by the symmetry, regardless of the physical context. Existence and stability results are found for even l up to $l=12$. Using either a variational or eigenvalue criterion, the preferred solution has icosahedral symmetry for $l=6$, $l=10$, and $l=12$. Numerical simulations of a model pattern-forming equation are in agreement with these theoretical predictions near onset and show more complex patterns further from onset.

DOI: 10.1103/PhysRevE.67.036206

PACS number(s): 89.75.Kd, 02.20.Qs, 02.30.Oz, 47.54.+r

I. INTRODUCTION

Pattern formation with spherical geometry arises naturally in a large number of physical and biological applications. Convection patterns in a spherical shell are relevant to continental drift driven by the fluid motion within the Earth's mantle. This problem has been studied analytically [1] and numerically [2,3] and a variety of solutions have been found, including some patterns with tetrahedral, cubic and icosahedral symmetry. Another physical application is the buckling of a sphere subjected to a uniform external pressure [4,5]. Biological applications include the growth of tumours, where a growing ball of cells may remain spherical or may bifurcate to a nonspherical shape [6,7], and the problem of morphogenesis in embryos, considered in the classic paper of Turing [8]. Reaction-diffusion equations have been solved numerically on the surface of a sphere [7,9], motivated by the formation of structure in viruses and tumours, generating essentially the same cubic and icosahedral patterns as found in the convection simulations.

This universality of patterns across different applications is a direct consequence of the spherical symmetry. The form of the bifurcation equations and the existence and stability of solutions with a particular symmetry is determined (in a sense made more precise below) purely by the fact that a bifurcation from spherical symmetry occurs. Considerable advances have been made in the mathematical theory of bifurcation with symmetry in the general case and in the specific case of spherical symmetry [10–13]. This paper provides further results on the existence and stability of patterns, and highlights a preference for icosahedral patterns.

II. DERIVATION OF EQUATIONS FROM SYMMETRY

At a bifurcation from spherical symmetry, the eigenfunctions are the spherical harmonics $Y_l^m(\theta, \phi)$ of degree l , for $-l \leq m \leq l$. The Y_l^m are proportional to $\exp(im\phi)$ and satisfy $Y_l^{-m} = (-1)^m Y_l^{m*}$. The value of l is determined by the problem; for example, in the case of spherical shell convection, l increases as the thickness of the shell decreases. There are $2l+1$ eigenmodes with the same growth rate, so the bifurcation equations are of order $2l+1$ and the problem becomes increasingly complicated as l increases. The $(2l+1)$ -fold degeneracy of the linear stability problem is

resolved by nonlinear terms. The cases of odd and even l are quite different [1,10]. For odd l , there are no quadratic terms in the bifurcation equations and so all bifurcations are of the pitchfork type. For even l , quadratic terms are present, so that all bifurcations are of the transcritical type; furthermore, there is a unique quadratic term that is consistent with the spherical symmetry [10] (up to an arbitrary amplitude scaling), so the behavior is uniquely determined. For this reason, only the case of even l is considered here.

Near a bifurcation point, the physical variable, for example, the temperature fluctuation in convection, is written as

$$W = \sum_{m=-l}^l z_m(t) Y_l^m(\theta, \phi), \quad (1)$$

where z_0 is real, z_m is complex for $m \neq 0$, and $z_{-m} = (-1)^m z_m^*$, since W is real. All the modes z_m have the same growth rate λ . Since there is a unique quadratic term that is consistent with spherical symmetry [10], this term can be obtained by computing W^2 and using orthogonality to extract the component in the equation for z_m . This leads to the system of $2l+1$ equations,

$$\dot{z}_m = \lambda z_m + \beta \sum_{m_1=-l}^l \sum_{m_2=-l}^l c(m_1, m_2, m) z_{m_1} z_{m_2}, \quad (2)$$

where $c(m_1, m_2, m) = 0$ if $m_1 + m_2 \neq m$, and

$$c(m_1, m_2, m) = \int_0^\pi \int_0^{2\pi} Y_l^{m_1} Y_l^{m_2} Y_l^{m*} \sin \theta d\phi d\theta \quad (3)$$

if $m_1 + m_2 = m$ and β is an arbitrary scaling parameter. The coefficients $c(m_1, m_2, m)$ are proportional to the Clebsch-Gordan coefficients

$$c(m_1, m_2, m) = \alpha \langle l, m_1, l, m_2 | l, m \rangle, \quad (4)$$

where the constant α depends on l .

III. EXISTENCE OF SOLUTIONS

The search for stationary solutions to the $2l+1$ equations (2) can be simplified by restricting attention to solutions with

TABLE I. Subgroups of $O(3)$ for even l , with corresponding number of equations $D(H)$. All solutions have an additional point inversion symmetry. $[x]$ denotes the integer part of x .

Group H	Symmetry	Elements	$D(H)$
$O(2)$	Circle	∞	1
I	Icosahedron	60	$1 - l/2 + [l/3] + [l/5]$
O	Cube	24	$1 - l/2 + [l/3] + [l/4]$
T	Tetrahedron	12	$1 - l/2 + 2[l/3]$
D_n	Regular n -gon	$2n$	$1 + [l/n]$
Z_n	Directed n -gon	n	$1 + 2[l/n]$

a particular symmetry. For example, if all the z_m are real, the solution has a reflection symmetry and the number of equations is reduced to $l + 1$. This symmetry can be described by a subgroup H of the original symmetry group of the sphere, $O(3)$. The subgroups of $O(3)$ are summarized in Table I, together with the corresponding dimension $D(H)$ of the restricted system, which can be computed using trace formulas. In fact, an additional point inversion symmetry is present for all solutions with even l . Since this symmetry is always present, it need not be explicitly written. The subgroups $O(2)$, corresponding to axisymmetric solutions, I representing solutions with icosahedral or dodecahedral symmetry, and O representing solutions with cubic or octahedral symmetry, are maximal, meaning that they are not contained in any other subgroup. The tetrahedral subgroup T is a subgroup of both I and O , and the dihedral group D_n is a subgroup of $O(2)$.

In the case $D(H) = 1$, the existence of solutions can be deduced from the equivariant branching lemma [11–13], which states that a branch of solutions with symmetry H exists near the bifurcation point. If $D(H) = 1$, then Eq. (2) reduces to the single equation

$$\dot{x} = \lambda x + ax^2, \tag{5}$$

where the constant a is in general nonzero, describing a transcritical bifurcation. The application of this result [11–13] shows that axisymmetric solutions [with symmetry $O(2)$] exist for all even l , solutions with symmetry O exist for $l = 4, 6, 8, 10, 14$, and solutions with symmetry I exist for 14 values of l .

A similar result for the case when $D(H) = 2$ can be obtained as follows. If $D(H) = 2$, the equations are

$$\dot{x} = \lambda x + ax^2 + bxy + cy^2, \tag{6}$$

$$\dot{y} = \lambda y + px^2 + qxy + ry^2, \tag{7}$$

involving six constants a, b, c, p, q, r . Multiplying Eq. (6) by y , Eq. (7) by x and subtracting yields a cubic equation for y/x at a fixed point, which in general has one or three solutions. Each of these solutions yields a unique solution for x and y after substitution back into Eqs. (6) and (7). Generically, there are therefore one or three branches of solutions when $D(H) = 2$. This result requires that certain nondegeneracy conditions are satisfied by the six constants in Eqs. (6) and

(7). It turns out that these conditions are satisfied for solutions with cubic symmetry O for the six cases in which $D(O) = 2$, so we may deduce the existence of either one or three branches of solutions with symmetry O for $l = 12, 16, 18, 20, 22, 26$. Similarly, we expect one or three branches of solutions with symmetry I for a further 15 values of l , simply by determining from Table I those l for which $D(H) = 2$. Extending this argument to the general case, it follows from Bezout’s theorem that generically, the number of solution branches is odd and less than or equal to $2^{D(H)} - 1$.

Demonstrating the existence of solutions with submaximal symmetry such as T and D_n is more difficult, since one must check carefully that the solutions obtained do not have greater symmetry. For example, for $l = 6$ and $l = 10$, $D(T) = 2$ and $D(O) = D(I) = 1$. Seeking solutions with symmetry T , the equations have the form (6), (7) but with a reflection symmetry so that $p = b = r = 0$. There are three solutions, but one of these has symmetry O and the other two have symmetry I and are equivalent under rotation. Therefore there is no solution with symmetry T for $l = 6$ or $l = 10$, as any such solution in fact has symmetry O or I .

For solutions with dihedral symmetry D_n , $D(D_n) = 2$ for $l/2 < n \leq l$, from Table I. Equations (2) then have the form

$$\dot{x} = \lambda x + \beta c(0,0,0)x^2 + 2\beta c(0,n,n)y^2, \tag{8}$$

$$\dot{y} = \lambda y + 2\beta c(0,n,n)xy, \tag{9}$$

where $x = z_0$ and $y = \text{Re}(z_n)$. There is an axisymmetric solution $y = 0$, $x = -\lambda/\beta c(0,0,0)$, and an additional solution

$$x = -\frac{\lambda}{2\beta c(0,n,n)}, \quad y^2 = \frac{\lambda^2}{4\beta^2 c(0,n,n)^2} \left[1 - \frac{c(0,0,0)}{2c(0,n,n)} \right],$$

provided that $c(0,0,0)/2c(0,n,n) < 1$. Using the properties of the Clebsch–Gordan coefficients, it has been shown [13] that this condition is met for $n = l$ if $l = 2 \pmod{4}$, since $c(0,0,0)/c(0,l,l)$ is proportional to $(-1)^{l/2}$ multiplied by a positive number. Further existence results can be obtained from the properties of the Clebsch–Gordan coefficients. It can be shown that

$$c(0,l-1,l-1)/c(0,l,l) = -(l-1)/2,$$

so that $c(0,0,0)/c(0,l-1,l-1)$ is negative if $l = 0 \pmod{4}$. Similarly,

$$c(0,l-2,l-2)/c(0,l,l) = (l^3 - 6l^2 + 3l - 2)/4(2l - 1),$$

which is positive for $l \geq 6$, and $c(0,l-3,l-3)/c(0,l,l)$ is proportional to a polynomial in l that is negative for $l > 10$. It follows that a solution with symmetry D_l exists for $l = 2 \pmod{4}$, $l \geq 6$ [13], a solution with symmetry D_{l-1} exists for $l = 0 \pmod{4}$, $l \geq 8$, a solution with symmetry D_{l-2} exists for $l = 2 \pmod{4}$, $l \geq 10$, and a solution with symmetry D_{l-3} exists for $l = 0 \pmod{4}$, $l \geq 12$. The constraints on l arise from the possibility of additional symmetry, for example a solution with symmetry D_4 may have symmetry O . It can be

shown that for large l , this pattern of existence of solutions continues, i.e. solutions with symmetry D_{l-2j} exist for $l=2(\text{mod}4)$, and solutions with symmetry D_{l-2j-1} exist for $l=0(\text{mod}4)$. Further details of these calculations are given elsewhere [14].

Stability of solutions is determined by the eigenvalues of the Jacobian matrix J . Earlier work [1,10] has established that Eqs. (2) have a variational structure, so that J is symmetric and hence all eigenvalues are real; furthermore, one of the eigenvalues is always equal to $-\lambda$ and the sum of the eigenvalues is $(2l+1)\lambda$ [10,13]. Hence all solutions are unstable near the bifurcation. However, there is always a solution in which, for $\lambda < 0$, one eigenvalue is positive and all the others are negative [10]. This can be regarded as a “preferred” solution since it can become stable at a saddle-node bifurcation if higher-order terms are introduced into Eq. (2). Alternatively, a variational formulation can be used [1], in which λ is maximized for a fixed value of the second-order invariant $\sum_{m=-l}^l |z_m|^2$; the solution that satisfies this variational problem also satisfies the above eigenvalue criterion [10]. Because of the spherical symmetry, zero eigenvalues are always present. The solution with $O(2)$ symmetry has two zero eigenvalues and all other solutions have three zero eigenvalues.

IV. SOLUTIONS FOR $l=6, 8, 10,$ AND 12

This section is concerned with calculation of the existence and stability of stationary solutions of Eq. (2) for specific even values of l . For $l=2$ the only solution is the axisymmetric state, while for $l=4$ there is an additional solution with symmetry O that is preferred, according to the variational or eigenvalue criterion [1,10,13].

For $l=6$, Busse [1] found four solutions, which have symmetry $O(2)$ (axisymmetric), I (icosahedral), O (cubic), and D_6 (hexagonal), and identified the solution with icosahedral symmetry as the preferred one according to the variational principle. These four solutions are guaranteed to exist by the general results above. As l increases, it becomes increasingly difficult to verify that all possible solutions have been obtained. For $l=6$, this can be done by investigating solutions with symmetry H for all possible subgroups H in the ‘lattice’ of subgroups. For the groups $O(2)$, I , and O , $D(H)=1$ and so a unique solution is guaranteed. For D_6 , D_5 , D_4 , and T , $D(H)=2$ and solutions can be found in each case; however, solutions with symmetry D_4 and D_5 give only the solutions with symmetry O and I , respectively, while solutions with symmetry T all have either symmetry O

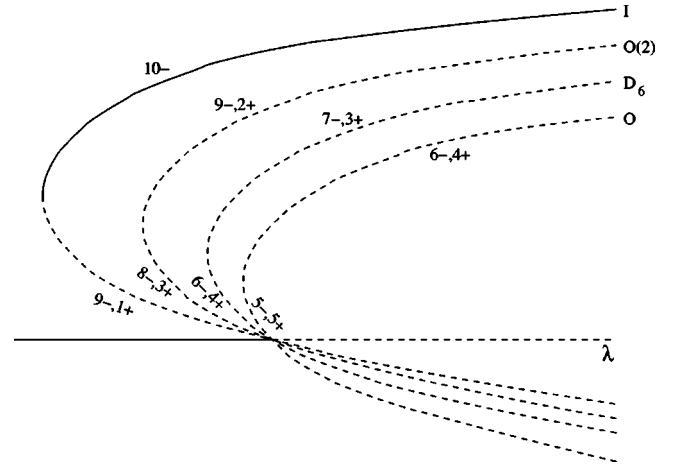


FIG. 1. Possible bifurcation diagram for the case $l=6$. Solid (dashed) lines denote stable (unstable) solution branches, and the vertical axis is a qualitative measure of the amplitude of the solution. The numbers of positive and negative eigenvalues on each branch are shown.

or I , so only D_6 gives a new solution. For the subgroup D_3 , $D(H)=3$ and there are seven solutions (in agreement with the above formula $2^{D(H)}-1$), but these are just copies of the solutions with symmetry I , O , D_6 and $O(2)$. Similarly, within the four-dimensional space of D_2 , there are $2^4-1=15$ solutions, but explicit computation verifies that there are no new solutions. Finally, solutions with symmetry Z_n , or no symmetry, can be ruled out since they are nongeneric [13].

It is straightforward to find the eigenvalues of the 13×13 matrix J for each solution, since J divides into blocks that are no larger than 3×3 . The eigenvalues and their multiplicities are shown in Table II. For the axisymmetric solution, the eigenvalues are simply $-\lambda$ and $[1-2c(0,n)/c(0,0,0)]\lambda$ for $n=1, \dots, l$, with multiplicity 2. One eigenvalue has multiplicity 4, since $c(0,2,2)=c(0,6,6)$. The other solutions also have eigenvalues with high multiplicity, up to 5 in the case of I .

The solution with symmetry I has only one positive eigenvalue for $\lambda < 0$, while all others have at least three. Hence the I solution can become stable at a saddle-node bifurcation if cubic terms are included, whereas the other solutions require more than one bifurcation to become stable. A possible bifurcation diagram illustrating this scenario is shown in Fig. 1. Note that only a single eigenvalue can change sign at a saddle-node bifurcation. On this basis, the I solution can be regarded as preferred. This supposition is given strong sup-

TABLE II. Eigenvalues of solutions for $l=6$, divided by λ . Numbers in parenthesis are multiplicities.

Symmetry	Eigenvalues
$O(2)$	$-\frac{7}{4} (2), -1, 0 (2), \frac{7}{5} (2), \frac{21}{10} (4), \frac{63}{20} (2)$
I	$-1, 0 (3), \frac{14}{11} (5), \frac{21}{11} (4)$
O	$-21, -\frac{21}{2} (3), -1, 0 (3), 7 (2), \frac{35}{2} (3)$
D_6	$-\frac{105}{22}, -\frac{35}{11} (2), -1, 0 (3), \frac{63}{22}, \frac{42}{11} (3), \frac{119}{22} (2)$

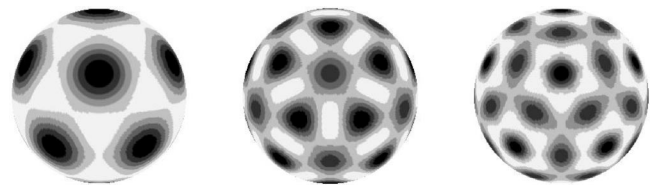


FIG. 2. Stationary solutions of Eq. (2) with icosahedral symmetry for $l=6, l=10,$ and $l=12$.

TABLE III. Solutions for $l=10$, with the number of equations $D(H)$ and the number of positive eigenvalues $n+$ when $\lambda < 0$.

Symmetry	I	$O(2)$	O	D_6	D_7	D_8	D_9	D_{10}	D_4	D_3
$D(H)$	1	1	1	2	2	2	2	2	3	4
$n+$	1	7	2	3	9	6	3	8	9	7

port by two recent numerical simulations of reaction-diffusion equations on the surface of a sphere [7,9], both of which find a stable solution with icosahedral symmetry for $l=6$. This question is examined further in Sec. V below. The solution with icosahedral symmetry is shown in Fig. 2. This solution has $z_0 = -\lambda/55$, $z_5 = \sqrt{77\lambda}/605$ and all other z_i are zero. In the example of spherical shell convection, the dark regions correspond to either warm rising fluid or cold sinking fluid, depending on the sign of β in Eq. (2).

For $l=8$, the equivariant branching lemma guarantees axisymmetric and cubic solutions, and the general arguments on solutions with symmetry D_n give a solution with symmetry D_7 . Direct computation reveals that there are also solutions with symmetry D_6 , D_5 , D_4 , and D_3 . There are no solutions with symmetry I or T . For $l=8$ there is a degeneracy in the coefficients, with $c(0,5,5)=c(0,6,6)$ and $c(1,5,6)=0$, these two equations being related by a recurrence relation of the coefficients. This degeneracy influences the eigenvalues of the solutions. The solutions with symmetry D_7 , D_6 , D_5 , D_4 , and D_3 all have seven zero eigenvalues, one positive eigenvalue and nine negative eigenvalues for $\lambda < 0$. It would therefore be necessary to include higher order terms to determine the preferred solution for $l=8$.

When $l=10$, solutions of Eq. (2) with symmetry $O(2)$, O , I exist, since these groups have $D(H)=1$. The other general results above indicate the existence of solutions with symmetry D_{10} and D_8 , and nonexistence of a solution with symmetry T . Calculations show that there are also solutions with symmetry D_9 , D_7 , D_6 , D_4 , and D_3 . These calculations follow the same general method as for $l=6$ and $l=8$; for each subgroup H of $O(3)$, $D(H)$ is obtained from Table I and the reduced set of $D(H)$ equations is solved. For submaximal subgroups, care must be taken to check whether the solution obtained has greater symmetry than H ; for example, when seeking solutions with symmetry D_5 , only the solution with symmetry I is found. Once a solution has been found, the eigenvalues of J are calculated for the full system of $2l+1$ equations. Some of the calculations were carried out using the symbolic algebra package MAPLE. The solutions are listed in Table III, with the number of eigenvalues that are positive when $\lambda < 0$. The I solution has only one positive eigenvalue for $\lambda < 0$ and so is regarded as the preferred solution. This solution is shown in Fig. 2.

For $l=12$, only the solutions with symmetry $O(2)$ and I are guaranteed by the equivariant branching lemma. The general result above for the case $D(H)=2$ shows that there are either one or three solutions with cubic symmetry O ; explicit computation of the coefficients in Eqs. (6) and (7) shows that in fact there are three distinct cubic solutions. For the other groups with $D(H)=2$, solutions with symmetry D_8 , D_9 , D_{10} and D_{11} exist but there are no solutions with symmetry D_7 or D_{12} . Solutions with symmetry T were investigated by restricting attention to solutions with symmetry D_2 that are also invariant under two consecutive $\pi/2$ rotations about orthogonal axes. The solutions with symmetry O and I were found, but also a distinct solution with symmetry T . Thus, $l=12$ is the lowest even value of l for which a solution with symmetry T exists. A total of 14 solutions were found for $l=12$; these are listed in Table IV. Again, the solution with symmetry I is preferred, since it has only one positive eigenvalue for $\lambda < 0$.

V. NUMERICAL SIMULATIONS

This section describes the results of numerical simulations of a model pattern-forming partial differential equation. The aim of the simulations is to test the hypothesis of the preceding section that the solution with only one positive eigenvalue for $\lambda < 0$ becomes stable at a saddle-node bifurcation and is the solution observed. The model chosen is a variation of the Swift-Hohenberg model,

$$\frac{\partial w}{\partial t} = [r - (1 + \nabla^2)^2]w + sw^2 - w^3. \tag{10}$$

This equation is widely used as a model for convection and other pattern-forming systems [15,16]. The basic state $w=0$ is potentially unstable when the parameter r becomes positive, and s represents the symmetry breaking between the inside and outside of the sphere. The growth rate λ of spherical harmonics of degree l is

$$\lambda = r - [1 - l(l+1)/R^2]^2, \tag{11}$$

where R is the radius of the sphere, so the most unstable mode has degree l if $R^2=l(l+1)$, in which case there is

TABLE IV. Solutions for $l=12$, with the number of equations $D(H)$ and the number of positive eigenvalues when $\lambda < 0$. Multiple entries in the final row indicate multiple solutions with the same symmetry.

Symmetry	I	$O(2)$	O	D_8	D_9	D_{10}	D_{11}	T	D_5	D_6	D_4
$D(H)$	1	1	2	2	2	2	2	3	3	3	4
$n+$	1	7	4,4,7	5	9	2	7	10	7	3	9,10

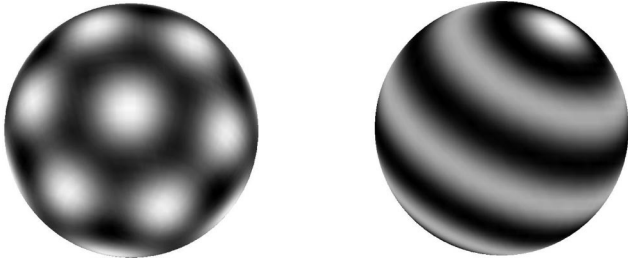


FIG. 3. Numerical solutions of Eq. (10) for $l=8$, with $r=0.15$, with symmetry D_6 (left) and $O(2)$ (right).

instability for $r>0$. Note that for large l the relationship between R and l is approximately $R=l+1/2$.

The simulations use a pseudospectral method, working with the spectral coefficients $z_{lm}(t)$ defined by

$$w = \sum_{l=0}^{l=L} \sum_{m=-l}^l z_{lm}(t) Y_l^m(\theta, \phi). \quad (12)$$

The number of modes L used is chosen to be at least three times the value of l with the maximum growth rate. The linear terms in Eq. (10) are obtained simply by multiplying z_{lm} by λ_l given by Eq. (11), and the nonlinear terms are found by transforming to a uniformly spaced grid in (θ, ϕ) on the surface of the sphere, evaluating w^2 and w^3 and then transforming back to the spectral coefficients. The transforms make use of the SPHEREPACK package [17]. The time stepping of Eq. (10) is carried out using the exponential time differencing method [18], which ensures that the exponential growth is handled exactly and allows much larger time steps than most standard methods. Each simulation employs a small-amplitude random initial condition.

To investigate patterns for $l=6$, several simulations with $R=6.5$, $s=0.2$ were carried out. For $r=0.1$, all random initial conditions lead to a stable solution with icosahedral symmetry, identical to that shown in Fig. 2. By choosing different initial conditions, with particular symmetries, the other three solutions shown in Table II can be found, but these are all unstable to small perturbations. These results are consistent with the bifurcation diagram sketched in Fig. 1, in which the branch of solutions with icosahedral symmetry turns round at a saddle-node bifurcation, giving a stable branch of solutions extending into the region where $\lambda>0$. This branch of solutions can be tracked back numerically into the region where $r<0$ (and hence $\lambda<0$) as far as $r=-0.0023$, before the solution collapses to the zero state, indicating that the saddle-node bifurcation occurs near this point. When r is increased to $r=0.2$, random initial conditions lead to either the icosahedral solution or the axisymmetric state, so both these solutions are stable, and for $r=0.3$ most initial conditions give the axisymmetric solution. This transition from an icosahedral solution with a pattern of spots to an axisymmetric striped pattern as r increases, with an interval of bistability, is closely analogous to the transition from hexagonal to striped patterns in planar pattern formation (see, for example, Ref. [16]).

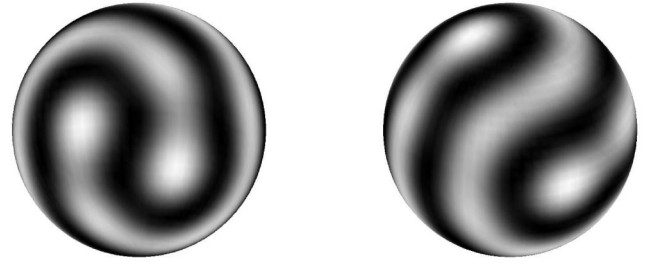


FIG. 4. Solutions of Eq. (10) for $l=8$, with $r=0.2$, showing a double-spiral pattern (left) and a tennis ball pattern (right).

For $l=8$, the theoretical results of Sec. IV based on the quadratic truncation do not give a preferred solution, since the quadratic terms do not resolve the pattern degeneracy in this case. Numerical simulations of Eq. (10) with $R=8.5$, $s=0.2$, $r=0.1$ show a pattern with D_6 (hexagonal) symmetry, with 20 spots on the surface of the sphere. For $r=0.15$, both the solution with D_6 symmetry and the axisymmetric solution are stable; these two solutions are shown in Fig. 3. For $r=0.2$, further stable solutions are found, depending on the initial conditions. These include, amongst others, a double-spiral pattern and a pattern with the symmetry of a tennis ball (Fig. 4). These two solutions do not have the point inversion symmetry inherent in all even- l states, and so are composed of a mix of even- l and odd- l modes.

For $l=10$, simulations with $s=0.2$, $R=10.5$, and $r=0.1$ generally lead to the solution with icosahedral symmetry shown in Fig. 2. However, a minority of initial conditions give an axisymmetric state, so it appears that both solutions are stable. For larger r , many different types of solution are stable. For $r=0.2$ these include the axisymmetric state, a double spiral similar to that of Fig. 4, and a single spiral pattern similar to that described by Zhang *et al.* [3] in their simulations of convection in a spherical shell.

Simulations with $s=0.2$, $R=12.5$, and $r=0.1$ (so that the most unstable mode is $l=12$) show either the icosahedral solution shown in Fig. 2, or the axisymmetric solution, or a solution with cubic symmetry, shown in Fig. 5, depending on the initial conditions. As r is increased, many more stable solutions are found, involving different arrangements of meandering stripes over the surface of the sphere. These include a double spiral similar to that found for $l=8$ and $l=10$, and a single spiral, shown in Fig. 5.

VI. CONCLUSIONS

In conclusion, this work represents a study of the existence and stability of solutions for pattern formation on a

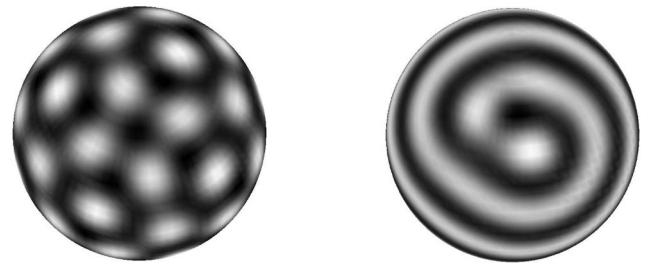


FIG. 5. Patterns in Eq. (10) for $l=12$. Cubic solution ($r=0.1$, left) and spiral solution ($r=0.2$, right).

sphere for all even l up to $l=12$. The bifurcation equations, to quadratic order, do not depend on the details of the physical application. All solutions found in the quadratic truncation are unstable, but a “preferred” solution can be identified using either a variational criterion or, equivalently, by determining which solution has only one positive eigenvalue. Remarkably, for $l=6$, $l=10$, and $l=12$, a solution with icosahedral symmetry is preferred, according to either the variational or eigenvalue criterion. These three solutions are shown in Fig. 2. Numerical simulations of a Swift-Hohenberg model confirm that these icosahedral patterns are indeed stabilized by higher-order terms, and show that a wide variety of more complicated patterns can be stable fur-

ther from onset. However, these higher-order terms are system dependent, so other pattern-forming equations may give different behavior.

The preference for icosahedral patterns is of considerable interest, since a very large number of “spherical” viruses are known to have icosahedral structures (see, for example, Ref. [19]), as first suggested by Crick and Watson [20]. For example, the bean pod mosaic virus and bacteriophage ϕ X174 both have the appearance of the $l=6$ solution of Fig. 2, while the turnip yellow mosaic virus and bacteriophage MS2 are similar to the $l=10$ solution, with 32 prominent surface features. A further natural example of icosahedral symmetry is in microorganisms known as radiolaria [21].

-
- [1] F.H. Busse, *J. Fluid Mech.* **72**, 67 (1975).
 [2] G. Schubert, G.A. Glatzmeier, and B. Travis, *Phys. Fluids A* **5**, 1928 (1993).
 [3] P. Zhang, K. Liao, and K. Zhang, *Phys. Rev. E* **66**, 055203 (2002).
 [4] G.H. Knightly and D. Sather, *Arch. Ration. Mech. Anal.* **72**, 315 (1980).
 [5] H. Pleiner, *Phys. Rev. A* **42**, 6060 (1990).
 [6] H. Byrne and P. Matthews, *IMA J. Math. Appl. Med. Biol.* **19**, 1 (2002).
 [7] M.A.J. Chaplain, M. Ganesh, and I.G. Graham, *J. Math. Biol.* **42**, 387 (2001).
 [8] A.M. Turing, *Philos. Trans. R. Soc. London, Ser. B* **237**, 37 (1952).
 [9] C. Varea, J.L. Aragon, and R.A. Barrio, *Phys. Rev. E* **60**, 4588 (1999).
 [10] D.H. Sattinger, *J. Math. Phys.* **19**, 1720 (1978).
 [11] E. Ibragimov and M. Golubitsky, *Physica D* **13**, 1 (1984).
 [12] M. Golubitsky, I. Stewart, and D. G. Schaeffer, *Singularities and Groups in Bifurcation Theory* (Springer, New York 1988).
 [13] P. Chossat, R. Lauterbach, and I. Melbourne, *Arch. Ration. Mech. Anal.* **113**, 313 (1990).
 [14] P.C. Matthews, *Nonlinearity* (to be published).
 [15] J.B. Swift and P.C. Hohenberg, *Phys. Rev. A* **15**, 319 (1977).
 [16] P.C. Matthews, *Physica D* **116**, 81 (1998).
 [17] J.C. Adams and P.N. Swartrauber, *Mon. Weather Rev.* **127**, 1872 (1999).
 [18] S.M. Cox and P.C. Matthews, *J. Comput. Phys.* **176**, 430 (2002).
 [19] N.J. Dimmock, A.J. Easton, and K.N. Leppard, *Introduction to Modern Virology* (Blackwell, Oxford, 2001).
 [20] F.H.C. Crick and J.D. Watson, *Nature (London)* **177**, 473 (1956).
 [21] D.W. Thompson, *On Growth and Form* (Cambridge University Press, Cambridge, 1942).